THESIS FOR THE DEGREE OF LICENTIATE OF ENGINEERING

Towards a mechanism for surface hydrophobization of paper
Effect of combinations of polyelectrolytes and polymer particles

FRIDA ISELAU

Department of Chemistry and Chemical Engineering

CHALMERS UNIVERSITY OF TECHNOLOGY

Göteborg, Sweden 2016

CHALMERS

Towards a mechanism for surface hydrophobization of paper

Effect of combinations of polyelectrolytes and polymer particles

FRIDA ISELAU

Licentiatuppsatser vid Institutionen för kemi och kemiteknik

Chalmers tekniska högskola

Serie Nr: 2016:09

ISSN: 1652-943X

Department of Chemistry and Chemical Engineering

Chalmers University of Technology

SE-412 96 Göteborg

Sweden

Telephone +46 (0)31-772 1000

Printed by Chalmers Reproservice

Göteborg, Sweden 2016

Towards a mechanism for surface hydrophobization of paper

Effect of combinations of polyelectrolytes and polymer particles

FRIDA ISELAU

Department of Chemistry and Chemical Engineering

Chalmers University of Technology

ABSTRACT

Paper materials are cost effective and light weighted, they can easily be recycled and their use as an alternative to plastics is advantageous from an environmental and sustainability perspective. However, competing with plastics for packaging applications is a challenge for cellulosic products. The material needs to be strong and stiff also when exposed to liquids or moisture during transportation and storage. To achieve this for paper materials, which are intrinsically hydrophilic due to the nature of the cellulose, they need to be hydrophobized.

Packaging paper materials are often made from recycled fibers. The constitution of the paper matrix can therefore vary a lot and the addition of hydrophobic compounds to the pulp in the paper production process is difficult to optimize. Therefore the recent development in paper hydrophobization has been towards surface modification, so-called surface sizing. There is a plethora of surface sizing products and these products are very efficient in making the paper surface more water resistant, but there is a lack of fundamental knowledge on *how* they work. The aim of this licentiate project, which can be regarded as the first part of a doctoral thesis work, is to explore and identify which physicochemical properties of the formulation used for surface sizing are governing the efficiency.

In surface sizing the particle suspension is first mixed with starch in solution. Starch is widely used to increase the surface strength of paper. The combination of the particles and starch is the subject of one study described in this thesis. In this study the interactions between starch and three types of particles, differing in the type of stabilizer used, are explored. The different stabilizers rendered the particles cationic, anionic or amphoteric. It was found that the cationic particles formed aggregates with the starch and that it is mainly the high molecular weight, highly branched amylopectin fraction of the starch that participates in the aggregation. The aggregate formation, as well as the relaxation kinetics, are also investigated and it was concluded that the amylopectin chains give rise to steric stabilization even at the most

destabilized state, i.e. at maximum aggregation. The relaxation kinetics is found to be molecular weight dependent while the equilibrated state is not, leading to a proposed aggregation mechanism based on patchwise flocculation.

Finally the efficiency in reducing the water uptake of test paper sheets is assessed. The cationic particles are the most efficient in decreasing the water uptake and the efficiency is enhanced by aggregation.

Keywords: Surface sizing, paper hydrophobization, aggregation, nanoparticles, starch, interactions, kinetics.

List of publications

I. **Role of the aggregation behavior of hydrophobic particles in paper surface hydrophobation**
Frida Iselau, Per Restorp, Mats Andersson, Romain Bordes
*Colloids and Surfaces A: Physicochemical and Engineering Aspects, 2015, **483**, 264-270*

II. **Competitive adsorption of amylopectin and amylose on cationic nanoparticles: a study on the aggregation mechanism**
Frida Iselau, Tuan Phan Xuan, Aleksandar Matic, Michael Persson, Krister Holmberg, Romain Bordes
*Soft Matter, 2016, **12**, 3388-3397*

III. **Formation and relaxation kinetics of starch-particle complexes**
Frida Iselau, Tuan Phan Xuan, Gregor Trefalt, Aleksandar Matic, Krister Holmberg, Romain Bordes
Manuscript

Contribution report

I. Responsible for all experimental work and the data analysis. Responsible for writing the manuscript.

II. Responsible for most of experimental work and the data analysis, except for the DLS and SAXS analyses. Responsible for writing the manuscript.

III. Responsible for most the experimental work and the data analysis, except for the DLS and SAXS analyses. Responsible for writing the manuscript.

1 TABLE OF CONTENTS

1. INTRODUCTION

For almost thousand years, since the Chinese invented the paper making process, paper has been an important part of our daily life. Already the ancient Egyptians, Greeks and Romans made paper from papyrus, hence the name "paper". During the industrialization the increased demand for paper lead to the development of the Fourdrinier machine, a continuous paper machine, which was patented in 1807. Many paper machines used today are based on the principles of the Fourdrinier machine.[1] Figure 1 describes schematically the paper making process.

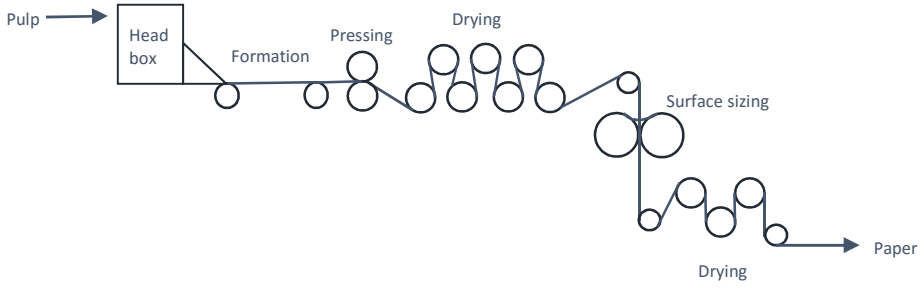

Figure 1. *Principles of paper making.*

With a world production of 400 million tons a year paper is an abundant and versatile material that has great value in everyday life.[1] It is used for communication in newspapers and magazines, for cleaning purpose as household paper, for writing and for printing. The many different applications require a toolbox of modifications of the naturally hydrophilic cellulosic fibers that are the main constituent in paper. A household paper should be very hydrophilic but yet strong in order to absorb liquid without losing its structure. A magazine paper should give excellent printability and print quality. Packaging is a growing market for the paper industry as more goods are transported across the continents. Paper as a packaging material fits very well the purpose as it is light, cost effective, and made from a renewable source. In addition, it can be recycled. A packaging material should be water resistant in order to withstand various storage conditions such as moist and liquid exposure without losing its strength or shape. Due to the intrinsic hydrophilic character of the cellulosic fibers these paper grades are hydrophobized to reduce penetration and wetting of water. However, water resistance is not needed only for packaging applications. To achieve good printability the paper surface needs to be hydrophobized in order to avoid ink

feathering.[2] In the paper manufacturing industry this treatment is frequently referred to as sizing. This word, used from historical times, is odd as its meaning is not straightforward. According to the literature the word "sizing" has three plausible origins.[3]

- Size could come from a word for glue because the first sizing method was done with glue. In Swedish and in French the word for sizing is still the word for "glue", i.e. in Swedish it is called "limning".
- Sizing might come from a test where a stack of paper was put in water and afterwards the increase in size due to water uptake was measured.
- The word "size" could stem from the old Latin verb "assidere". Early Italian papermakers called the procedure "assisa" which can have been modified to "sisa" and then to "size". It means "set in place."

Historically, the first sizing method was surface sizing. It was achieved by wetting the handmade paper sheet through a pond containing the surface sizing ingredients. With this method, there was no tension affecting the paper's durability. Later, when the paper machines were introduced, the tension on the paper web going through the machine was significantly increased and therefore the paper web often broke due to too high water uptake in the size pond. To solve this problem internal sizing was developed.

Internal sizing is typically done by adding hydrophobic, reactive compounds like alkyl ketene dimer (AKD) and alkenyl succinic anhydride (ASA) to the pulp. These compounds react with the cellulosic chains, forming covalent bonds and rendering fiber surfaces more hydrophobic.[4-7] This is done before the pulp is formed into a paper giving the entire bulk of the paper a hydrophobic character. The efficiency of the internal sizing process is depending on different factors and the procedure suffers from various shortcomings. For instance, it is important to have good retention of the internal sizing agent, i.e. the compound must be retained in the pulp and not drained off with the recirculating water flow. This is essential since both AKD and ASA are susceptible to hydrolysis and will degrade if the residence time is too long. Therefore the use of an efficient retention aid is crucial and the pH needs to be on the neutral/basic side in order to avoid hydrolysis. A high filler and/or fines content, as for example in fine paper and recycled paper grades, is detrimental for internal sizing since the hydrophobizing agent is then adsorbed on the small particles/fibers and not on the long, strong fibers. With a high fines content a higher dosage of internal sizing agent is therefore needed.

For technological, economic and environmental reasons, there is currently a shift engaged from internal sizing to surface sizing.[8] In surface sizing, the hydrophobizing agents are applied in the dry-end of the paper machine onto the formed paper sheet (see Figure 1). They are therefore mainly present at the paper surface, where they are primarily needed, allowing a significant reduction of the amount of chemicals used in the hydrophobization process. Surface sizing has the additional advantage of having efficient retention[9-12] which is beneficial both from an economic and a process runnability point of view.[11] Technical reasons also favor surface sizing over internal sizing. For instance, for recycled paper, where the composition may vary a lot, efficient internal sizing is often difficult to achieve.[9]

In surface sizing the paper material is typically treated with a suspension of hydrophobic polymer particles in a starch solution.[10, 11, 13, 14] The starch enhances the paper stiffness by forming a film on the paper surface that creates strong hydrogen bonds with the cellulose fibers[12] and can also reduce the water penetration rate by filling the surface voids in the paper sheet.[11] In surface sizing the starch is dissolved and held at elevated temperature in order to decrease the risk of retrogradation. The hydrophobic polymer particles, typically a styrene-acrylate based copolymer, stabilized by amphiphiles of different nature,[14-17] render the paper surface hydrophobic.[11, 13, 15, 18, 19] The particle suspension is first mixed with the starch solution and the mixture is subsequently applied on the paper surface at the dry-end of the paper machine.[20] A pressure is applied and the paper is usually heated above the glass transition temperature of the polymer in order to promote coalescence of the colloidal layer.[16] There are different techniques to industrially apply the particles on the surface of the paper, the most important being puddle press and film press.[11] For both techniques, the paper is first exposed to the particle/starch suspension to allow liquid absorption and adsorption to take place, and then, exposed to an external pressure, the press step. This is followed by the drying step. Figure 2 shows a schematic description of surface sizing at laboratory scale.

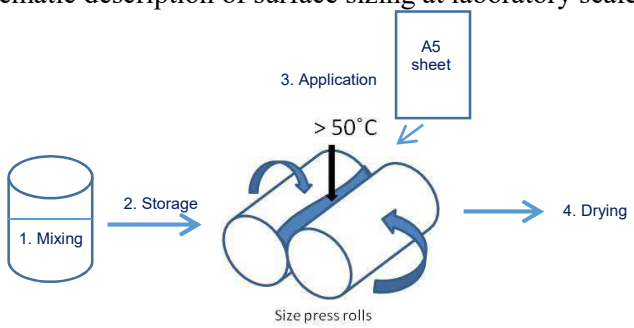

Figure 2. *A schematic representation of the surface sizing procedure.*

Surface sizing polymer suspensions are widely used in the paper making industry today and there is a variety of grades differing in particle size, colloidal charge and chemical composition, in order to fine-tune the hydrophobization process. The various grades are known to be very efficient. Only a small addition of these hydrophobic polymer particles will render the paper surface hydrophobic. However, most of the knowledge is empirical and it is generally accepted in the paper industry that there is a lack of fundamental knowledge of how these products work. It is also not known which properties of the paper sizing formulation are governing the performance.

In this study the importance of the colloidal behavior of the hydrophobic particles in combination with anionic starch was explored and correlated to surface sizing performance. Three different particle types were synthesized with the same hydrophobic polymer core but with different stabilizers (dispersants). Depending on the stabilizer the particles are either cationic, anionic or amphoteric and are here labelled SP+, SP- and SPA, respectively. The particle concentration was typically 0.1 wt% and the starch concentration was 8 wt%, i.e. a high starch to particle ratio was used, which is in line with industrial conditions. Even in the strong excess of anionic starch a difference in performance could be seen when comparing the three formulations, showing that in spite of having the same hydrophobic core the nature of the stabilizer played a significant role for the hydrophobization. The interactions introduced in Paper I and further explored in Paper II and Paper III could be correlated to an improved efficiency in surface hydrophobization when optimal conditions were applied. The conclusions from this study, that the starch to particle ratio, the temperature, and the molecular weight of the starch are decisive for the aggregation and consequently for the surface sizing efficiency give a new insight and deeper understanding of the mechanism of surface sizing.

2. OBJECTIVES

The aim of this PhD project is to gain deeper understanding of the fundamental principles of surface sizing. One may say that there are as many applications and variations on surface sizing as there are paper mills in the world; however, the basic principles of surface sizing are generic. The scheme of the surface sizing procedure shown in Figure 2 can be divided into four steps:

1. Mixing of components
2. Storage of mixture
3. Application
4. Drying

Together, these steps will lead to a hydrophobized paper surface and it is therefore important to evaluate the whole process in order to identify the crucial parameters for achieving the optimal sizing effect. The effect of mixing the components and of storage of the mixture are investigated in this licentiate thesis. Further studies, which are beyond this thesis, will provide insights of the application and the film forming process during drying.

3. ANALYTICAL TECHNIQUES

The complexity of the systems studied in this work is reflected by the diversity and the broad range of analytical techniques employed. For the bulk study of the formulations, scattering techniques that range from turbidity to SAXS gives information about the overall behavior of the colloidal system as well as the internal structure of the aggregates formed. The paper surface characterization includes both physical and chemical analytical techniques since the paper surface is structured and has a heterogeneous nature.

3.1. SCATTERING TECHNIQUES

When a radiation beam is illuminating a sample, the beam is scattered. The scattering pattern is the result of the inhomogeneity of the sample. The scattered beam is monitored by detectors and the intensity of the scattered beam as a function of the angle of detection is measured. Examples of radiation sources are light (laser) or X-rays.[21] Depending on the wavelength source, different size ranges can be measured where the X-ray provides analysis of samples in the lower nano size range while light scattering can be used for size determination ranging from 10 nm to 1 μm.

Scattering techniques provide a non-invasive measurement of macromolecules and particles in solutions or dispersions. From scattering measurements information about size, molar mass, radius of hydration, radius of gyration and form factor can be extracted. The theory of Rayleigh states that the scattering intensity is proportional to the power of six of the particle size means that the larger the particle the higher is the scattering intensity.[22]

3.1.1. Turbidity

When light passes through a particle suspension the incoming beam is scattered due to interactions with the matter. When the particle size is smaller than the incoming wavelength of the light the turbidity increases with particle size.[21] Turbidity can be used for monitoring size growth due to aggregation, however not quantitatively. A UV/Vis spectrophotometer can be used for turbidity measurements where incoming light in the UV and visible spectra, from 200-800 nm is illuminating the sample. The intensity of the transmitted light is monitored and its decrease is the results of the presence of aggregates and of their size.

3.1.2. Static light scattering, SLS

Static light scattering, SLS, is a scattering technique that can be used to determine the molecular weight, M_w, and the form factor, $P(\theta)$, from which the radius of gyration, R_G, can be obtained. In SLS a polarized laser light with known intensity is illuminating the sample and the intensity of the scattered light is measured over a period of time, typically 10-30 seconds. The accumulation of the scattering intensity over a period of time gives the time-averaged intensity where the fluctuations are removed and this is why the technique is called *static* light scattering. The form factor describes the dependence of the intensity on the scattering wave vector (q) and depends on the structure and the size of the solute. Often multiple detectors placed at different angles around the sample holder are used for the detection, this technique is then called Multiple Angle Light Scattering, MALS. The use of multiple detectors improves the accuracy in the measurements.

3.1.3. Dynamic light scattering, DLS

In a dispersion, the solvent will have an impact on the particles causing them to move, the so-called Brownian motion. Dynamic light scattering, DLS, is a scattering technique where the time-dependent fluctuation in the scattering from moving particles due to Brownian motion is monitored. The fluctuation is correlated to the diffusion rate of the particle in the solvent and the diffusion rate is in turn correlated to the hydrodynamic radius of the particle. The hydrodynamic radius (R_H) can be calculated from the average diffusion coefficient using the Stokes-Einstein equation (Eq. 1):

$$D = \frac{kT}{6\pi\eta R_H} \quad \text{(Eq. 1)}$$

Where η is the viscosity, k is the Boltzmann's constant and T is the absolute temperature. The radius of hydration, R_H, that is obtained from DLS is for a sphere always larger than the radius of gyration, R_G, obtained from SLS.

3.1.4. Small angle X-ray scattering, SAXS

In small angle X-ray scattering, SAXS, an X-ray beam is employed for irradiation of a sample. The X-ray is interacting with the electron shell of the atom and the fluctuations in the electron density gives elastic scattering. The intensity of the scattering is in turn detected. The sample can be in solid state or as a dispersion. The term small angle is due to the small deflection of the scattering radiation, which is often between 0.1-10 °. SAXS is used for size and shape determination and it also gives information about the inner structure of disordered systems. SAXS can be seen

as an extension of SLS, where the smaller wavelength of the incoming X-ray beam can be used for size determination in the Å regime.

With SAXS the scattered intensity and the scattering angle is monitored. The scattering angle is used for calculation of the scattering vector, q, by the relation (Eq. 2):

$$q = \left(\frac{4\pi}{\lambda}\right) sin\theta \qquad \text{(Eq. 2)}$$

The log-log plot of the scattered intensity as a function of the scattering vector gives the fractal dimensions of the measured system. A non-aggregated systems constitutes of one structural level and the size can be determined from the Guinier approximation,[23] (Eq. 3):

$$I(q) = I_0 exp\left(\frac{-R_G^2 q^2}{3}\right) \qquad \text{(Eq. 3)}$$

A structural level in scattering is described by Guinier's law and a structurally limited power law, which on a log-log plot is reflected by a kink and a linear region. For complex systems a unified equation can be used to model the scattered intensity.[24] This is an approximated term that describes a complex morphology over a wide range of q in term of structural levels. Intensity is modelled using the formula (Eq. 4):

$$\mathrm{I(q)} = \sum_{\mathrm{i=1}}^{\mathrm{n}} \mathrm{G_i}\ \exp\left(\frac{-\mathrm{q^2 R_{Gi}^2}}{3}\right) + \mathrm{B_i} \exp\left(\frac{-\mathrm{q^2 R_{G(i+1)}}}{3}\right) \times \left[\frac{\left(\mathrm{erf}(\mathrm{qR_{Gi}}/\sqrt{6})\right)^3}{\mathrm{q}}\right]^{\mathrm{P_i}} \qquad \text{(Eq. 4)}$$

where n is the number of structural levels, i=1 refers to the largest size structure, and (i+1) to the structure of the sub-particle. G is the Guinier prefactor and B is a prefactor specific to this type of power-law scattering. B is defined according to the regime in which the exponent P falls. Generally, for surface fractals $4 > P > 3$, for mass fractals $P < 3$ and for diffuse interfaces $P > 4$.

3.2. ELECTROPHORETIC MOBILITY AND ζ POTENTIAL

A charged particle suspension has a distribution of counter-ions surrounding the particle surface. Close to the surface the counter-ions are strongly bound and this is defined as the Stern layer. Outside the Stern layer there is still a higher ion concentration compared to the bulk but the ions are less firmly bound to the particles. This layer is called the diffuse layer. When a voltage is applied to a particle suspension an electric field is created and the particles are attracted to the electrode

of opposite polarity. The particle velocity in this electric field can be measured and from this the electrophoretic mobility can be calculated from the relation $\mu_e = v/E$, where v is the velocity and E is the applied electric field.[25] The velocity is measured by electroacoustic or laser Doppler electrophoresis techniques. The detection for the instrument used in this study was laser Doppler electrophoresis which utilized the Doppler effect, i.e. that a moving object will induce a phase shift in frequency.[26] By comparing the frequency of the scattered light with the incoming light frequency the velocity can be calculated. The electrophoretic mobility depends only on the amount of charge carried by the particle and not on the particle shape or size.[27]

When the external voltage is applied to the particle suspension the ions bound to the particle surface will move along with the particle. At a specific distance from the particle surface, inside the diffuse layer, there is a limit where the ions no longer follow the particle's movement. This is called the slipping plane. The potential at this border is defined as the ζ potential and can be calculated by the Smoluchowski formula where the ζ potential is obtained from the viscosity of the solution, the dielectric constant and the electrophoretic mobility.[25] The ζ potential therefore reflects the effective particle charge and is the potential in the electrical double layer that exists between the particle surface and the surrounding medium, often water. The ζ potential is dependent on solution conditions such as pH and ionic strength, and the ζ potential measurements should preferable be performed with a constant background electrolyte concentration.

3.3. COBB TEST

The Cobb test is a water absorptiveness measurement on sized paper and a TAPPI standard method.[28] In this test the water absorptiveness, i.e. the Cobb value, is defined as the mass of water absorbed in a specific time by 1 m^2 paper under 1 cm of water and given in the unit g/m^2. The exposure time is often 60 seconds but for specific requirements also longer times can be employed, for example Cobb1800 which corresponds to an exposure time of 1800 seconds. The lower the Cobb value the better is the water resistance of the tested surface. A Cobb value below 30 g/m^2 is usually regarded as a sufficient sized paper surface.

4. MATERIALS AND METHODS

4.1. MATERIALS

The particles used in this study, e.g. the SP+, SPA and SP- were synthesised as described in paper I. Also used in this study was amidine latex particles (AL110) from Invitrogen (Basel, Switzerland).

For the study of colloidal behavior two starch types were used, one oxidized potato starch and one oxidized waxy potato starch. The starches were supplied as dry powders from Avebe, Holland.

The test papers used in the sizing efficiency assessment were a fine paper grade and a recycled liner grade. The fine paper was produced on a pilot paper machine at the Technical University of Munich. The composition of the fine paper grade was chemical pulp with a filler content of ground calcium carbonate (GCC) corresponding to an ash content of 16-18 %. Alkyl ketene dimer, AKD, was used as internal sizing agent and a cationic starch, Vector IC, from Roquette with a DS of 0.03 was used for mechanical strength enhancement. The liner grade was from Mintec and consists of 100 % recycled fibers and was not internally sized.

4.2. ANALYTICAL METHODS

4.2.1. Characterization methods

4.2.1.1. Particle size determination

A Malvern Nano instrument was used for measuring the particle size by dynamic light scattering for SP+, SPA and SP-. The samples were prepared by diluting the particles in Milli-Q water to a concentration of 0.05 wt%. Samples were filtrated with 0.2 µm hydrophilic syringe filter (Sartorius) before measurements.

4.2.1.2. ζ potential

The ζ potential was measured using a Malvern Nano instrument and disposable measuring cells and was calculated using the in-build software that employs similar models as for phase analysis light scattering.[30]

The ζ potential for the SP+, SPA and SP- particle suspensions was measured and the samples were prepared by diluting the particle suspension to a concentration of 0.05 wt% with a 1 mM NaCl solution. The samples were filtered with 0.2 µm hydrophilic syringe filter (Sartorius) before measurement.

For the ζ potential measurements of the cationic particle suspension in combination with the anionic starch the SP+ concentration was 0.1 wt% and a 3 wt% starch solution was added in different amounts to the particle suspension. Both the SP+ and the starch were filtered with 0.2 µm hydrophilic syringe filter (Sartorius) before mixing. The samples were analyzed 5 min after the starch addition and no background electrolyte was used. pH remained constant throughout the titration around 4.0.

4.2.1.3. Particle charge density titration

Particle charge density titration was performed with oppositely charged polymers using a Particle Charge Detector (PCD), CAS Charge Analyzing System (AFG, Analytic GMBH). This is an electrokinetic technique where the charge distribution is determined by measuring the streaming potential.[31, 32] The amount of surface charge is determined by the titration of the suspension with a titrant carrying the opposite charge and the amount of titrant required for charge neutralization at a macroscopic level is used for calculating the charge density. For the anionic SP- particles the titration was performed using polyDADMAC and for the amphoteric, SPA, and cationic, SP+, particles the titration was performed with PES-Na. The

anionic starches, the regular and waxy starch, were titrated with polyDADMAC. The samples were filtered with 0.2 µm hydrophilic syringe filter (Sartorius) before measurement. Charge titrations of the SP+ particles with the anionic regular or waxy starch as the titrants were also performed in order to investigate the starch to particle ratio at charge neutralization.

4.2.1.4. Freeze fracture with transmission electron microscope (TEM)

The samples were prepared by the freeze fracture mica method and then high resolution TEM pictures could be taken. In this method a small amount of a diluted sample is placed in between two mica plates and rapidly frozen in liquid nitrogen. The mica sandwich is split up and the surface now covered by a frozen particle suspension is placed in a holder, still in liquid nitrogen and placed in the vacuum chamber. In the chamber the temperature was -170 °C to allow water sublimation. The surface is then covered by a platinum layer, 0.8 nm thick, and a 2 nm carbon layer. The carbon layer worked as a support for the thin platinum layer. The reproduction of the sample structure was then studied by TEM. The three particle types SPA, SP- and SP+ at concentrations of 0.05-0.07 wt % were included in the study.

4.2.2. Methods to study colloidal stability

In the surface sizing process the hydrophobic polymer particle suspension is mixed with a starch solution prior application on the paper web surface. A study was performed in order to investigate the colloidal behavior for the three different particle types in the presence of starch, in this case an oxidized starch that has anionic character. The colloidal behavior was primarily studied by turbidity and further investigated by light scattering, ζ potential and SAXS. The molecular weight of the starch in solution after mixing with the particles was analyzed by SEC.

4.2.2.1. Turbidity

The turbidity measurements were performed on an Agilent Cary 60 UV/Vis instrument and HP8453 UV/Vis instrument using a quartz cuvette or disposable acrylic cuvettes. The baseline was recorded in Milli-Q water. The value of the absorbance at 400 nm was used as a measure of the turbidity. The particle suspension, 0.1 wt%, was filtered with 0.2 µm hydrophilic syringe filter (Sartorius) before 2 mL sample was transferred to the cuvette. The starch solution was also filtered with 0.2 µm hydrophilic syringe filter (Sartorius) before addition to the particle suspension. For the relaxation kinetics study eight samples, with different amount

starch added to the particle suspension, were measured simultaneously for a period of time. The turbidity measurements at elevated temperature were done using the HP8453 UV/Vis instrument that was equipped with a temperature controlled sample holder. To avoid cooling the sample by the addition of starch, the starch solution was preheated in a water bath.

4.2.2.2. Aggregate size determination by light scattering

For the size determination of the formed aggregates a multi angle light scattering instrument, ALV/CGS-8F, was used. The instrument was equipped with a laser source of 150 mW with a wavelength of λ= 532 nm. The temperature was controlled by a thermostat bath to within ± 0.2 °C. Measurements were made at angles of observation (Θ) between 12 and 155 degrees. From these measurements both R_H and R_G were determined. The particle concentration was 0.05 wt% and different amount of a 3 wt% starch solution was added to the particle suspension. Both the particle suspension and the starch were filtered with 0.2 µm hydrophilic syringe filter (Sartorius) before mixing. After 5 min the samples were analyzed. Details of the data processing are further explained in paper II and III.

Starch has a much lower scattering intensity compared to the particles. Therefore the scattering intensity detected in the measurements of the mixture of particles and starch is regarded to originate from the aggregates. The slightly increase in sample viscosity due to starch addition was minor and was therefore assumed not to affect the results.

4.2.2.3. Aggregate formation

Early stages of aggregation of AL110 particles as a function of starch concentration were studied using ALV/CGS-8F goniometer. The samples were prepared by mixing appropriate amounts of stock suspension of 0.02 wt% of AL110 particles with 0.005 wt% of starch solution. Background electrolyte concentration was adjusted by adding aqueous NaCl solution. Final concentration of particles in the mixture was kept at 0.00072 wt%. Immediately after mixing, the hydrodynamic radius *vs* time was monitored with the DLS, where R_H was calculated from the second order cumulant fit. The stability ratio W was calculated by comparing actual apparent aggregation rate coefficient, k_{app}, with the one measured in 930 mM NaCl without added starch, k_{fast}, where $W = k_{fast}/k_{app}$.

4.2.2.4. SAXS

Small angle X-ray scattering, SAXS, experiments were carried out at the I911-4 beamline of the MAX-Lab laboratory synchrotron using a wavelength of 0.91 Å. The samples were analyzed for 120 s in capillaries maintained at 20 °C. Depending on the analysis of interest the samples were prepared right before the measurements (kinetic study) or 24 h prior analysis. The samples were prepared by adding different amounts of the 3 wt% starch solution to samples of 2 mL of a 0.1 wt% SP+ suspension. The particle suspension and the starch solution were filtered with 0.2 µm hydrophilic syringe filter (Sartorius) before addition.

4.2.3. Paper characterization methods

Two types of model papers were used, one recycled liner grade and one fine paper grade. The test papers were characterized with respect of porosity and water uptake both for untreated paper sheet as well as on surface sized paper sheets. For the untreated paper sheets the charge and chemical composition of the material have been determined.

4.2.3.1. Chemical composition of the paper surface

X-ray photoelectron spectroscopy, XPS, was used to determine the chemical composition of the paper surface. A Quantum 2000 scanning XPS microprobe from Physical Electronics with an Al Kα (1486.6 eV) X-ray source was used with a beam size of 100 µm. The analyzed area was 500 x 500 µm and the take-off angle was 45 ° with respect to the sample surface. The information depth is approximately 4-5 nm.

4.2.3.2. Air permeability and roughness

The air permeability and roughness were measured using a Bendtsen equipment where pressurized air is flowed through the paper sheet for determination of air permeability and along the paper surface for determination of surface roughness. The air permeability is dependent on the paper thickness as well as the porosity of the paper sheet. Both the air permeability and roughness are given in the unit mL(air)/min. Typically, a low flow indicates that the paper surface is smooth while a high flow is a sign of roughness.

4.2.3.3. Colloidal charge of fiber slurry

To measure the colloidal charge of the fiber slurry approximately 30 g of paper sheets were grated into small pieces and added to 2000 mL deionized water and let to swell for two hours. The swelled paper fragments were then defibrillated using a blender.

Afterwards the dry content was measured and the slurry was diluted to a final concentration of 4 g/l. The fibre charge was measured with PCD. The pH of the slurry was measured before and after titration. As titrand polyDADMAC 0.001 N was used.

4.2.3.4. Cobb 60

The surface sizing performance was evaluated with the Cobb 60 method according to TAPPI Method T-441. In short it is a weight water pick-up test where 100 mL of deionized water is applied onto a 100 cm^2 area of the paper surface during 60 seconds using a retaining ring that is clamped on top of the paper. After 60 seconds the excess of water is removed and the water uptake is measured as a weight increase of the paper sheet.[16]

4.2.3.5. Scanning electron microscope, SEM

The paper surfaces were analyzed with Scanning Electron Microscopy, SEM, using a Leo Ultra 55 FEG SEM (Leo Electron Microscopy Ltd, Cambridge, UK) microscope. The paper samples were sputtered with gold with an Edwards S150B Gold Sputter Coater.

4.2.3.6. Surface sizing test method

The oxidized starch solution used for the surface sizing tests was prepared in a jet batch cooker where high temperature, high pressure and high shear forces from the steam gives a fully hydrated starch in solution.[34] The final starch solution was held at approximately 70 °C during storage to prevent retrogradation[11] and around 60 °C when used in the test. The hot starch solution was added to a specific amount of hydrophobic particle suspension and the mixture was diluted to a final concentration of 8 wt% starch and 0.02-0.2 wt% particles. The mixture was then applied in a size press laboratory equipment from Mathis AG. During application the liquid temperature was held above 60 °C. The test papers were put in between the size press rolls and transported through the pond and the surface sizing mixture was pressed into the test paper. The surface sized paper sheets were dried in a contact dryer held at 80 °C. The surface sized paper sheets were then placed in a climate room with a temperature of 23 °C and relative humidity of 50 % overnight. The hydrophobic resistance was evaluated after 24 h by the Cobb 60 test method.

5. CHARACTERIZATION OF THE PARTICLES, THE STARCHES AND THE TEST PAPERS

5.1. THE HYDROPHOBIC PARTICLES

5.1.1. Particle composition

In this research work three particle types have been synthesized where the composition of the particles is the same, 60 wt% hydrophobic polymer in the core and 40 wt% stabilizer. All three particle types have the same hydrophobic co-polymer core; a copolymer of styrene and butyl acrylates, but they differ by the type of stabilizer. The particle type called SP+ has a cationic, synthetic polymer as stabilizer. The SPA type has a cationized, oxidized starch as stabilizer and the SP- type is stabilized by an oxidized starch. A schematic view of the particles is shown in Figure 3.

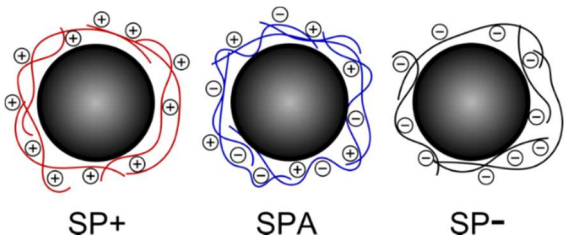

Figure 3. *Colloidal stability is achieved by a cationic, amphoteric or anionic stabilizer, as illustrated in this figure.*

5.1.2. Particles synthesis

The cationic stabilizer used in this study is a copolymer of styrene and quaternary ammonium monomers. The anionic and amphoteric stabilizers are starch-based materials (oxidized or cationizied respectively) where the starch first was oxidatively degraded by the redox system hydrogen peroxide/iron-(II)-sulphate.

The radical polymerization was carried out as an emulsion polymerization in the presence of the stabilizer (degraded starch or synthetic copolymer). The polymerization was initiated by hydrogen peroxide in presence of iron-(II)-sulphate

that acts as a catalyst for formation of radicals. To control the molecular weight, dodecanethiol was used as a chain transfer agent.

5.1.3. Particle characterization

The particles were characterized using several analytical tools as well as imaging techniques. The particle size, the ζ potential, the colloidal charge and the glass transition temperature are listed in the Table 1 below.

Table 1.

Hydrodynamic diameter, ζ potential, surface charge and glass transition temperature of the three polymer particle types.

	Particle diameter (nm)	ζ potential (mV)	PCD titration (μeq/g)	Tg (°C)
SPA	75	-2	8	73
SP-	76	-29	-60	74
SP+	41	45	560	70

The particles prepared in the presence of the starch based stabilizers have similar sizes, close to 75 nm. The SP+ particles prepared with the cationic synthetic emulsifier are smaller, around 40 nm as a result of the higher effectiveness of the emulsifier.

The effective charge of the particles is reflected by their ζ potential and further information about the particle charge is provided by colloidal charge titration using a particle charge detector equipment (PCD). The charge of SP-, where an oxidized starch is used as stabilizer, is strongly anionic as can be seen in Table 1 where both the ζ potential and the colloidal charge are negative. This is due to the formation of carboxylic groups in the oxidation reaction of starch carried out prior to the polymerization as well as during the synthesis.

The amphoteric particles, SPA, are stabilized by a starch that carries both cationic charges from quaternary ammonium groups as well as anionic charges from the oxidation of the starch during the degradation step and further oxidation also occurs during the particle synthesis. As can be seen in Table 1 the SPA particle is therefore almost neutral. A slight difference can be noted between the ζ potential measurement and the PCD, which can be attributed to the measurements conditions since the ζ potential is measured in a 1 mM NaCl solution while the PCD titration is performed

in deionized water. As expected, the SP+ particles prepared with the cationic synthetic stabilizer have a pronounced positive ζ potential and colloidal charge.

The particle synthesis was repeated for all three particle types to assess variations in the synthesis routine. The reproduced particle batches were found to have similar properties and the overall behavior was the same.

The glass transition temperature for the three particle types is also listed in Table 1. Regardless of the synthesis route, the values obtained are around 70 °C. This is important since the glass transition temperature of the hydrophobic polymers in the particle core will govern the flexibility of the polymers upon heating which in turn can affect the sizing efficiency and the film forming process.

Freeze fracture TEM was employed for imaging of the surface sizing particles, SP+, SPA and SP- and the TEM pictures of the particles (Figure 4) confirmed the particle sizes determined by DLS. The pictures also revealed different behavior on the slightly anionic charged mica surface. The sample preparation for SP- was more difficult as there was repulsion between the anionic particles and the mica surface and therefore the imaging of SP- was unsuccessful. The cationic particles, SP+, were evenly distributed on the mica surface due to attraction to the surface and repulsion between the individual particles. The amphoteric particles that have almost no net charge showed a more random distribution on the surface.

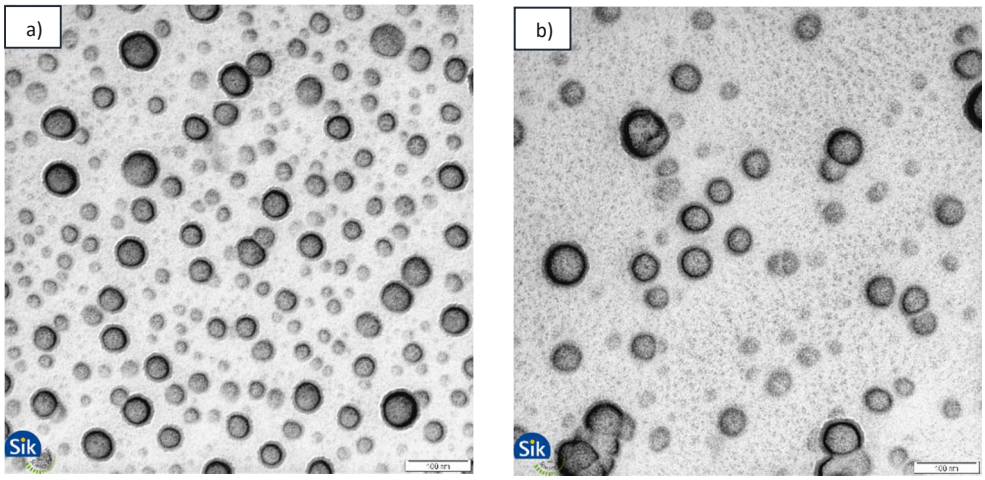

Figure 4. *TEM pictures of a) SP+ particles and b) SPA particles.*

The SAXS analysis of the SP+ particles gave a radius of gyration for the SP+ particles of 14 nm. The value of $P = 3.8$ showed that the particle presents a rough fractal

surface. This can be explained by the core-shell structure of the SP+ particles where the polymeric stabilizer acts like polymer brushes on the surface.[35]

5.2. STARCH

The starch contributes to the paper stiffness[12] by increasing the surface strength of the paper and it decreases the rate of water uptake by providing a smoother surface. However, due to its intrinsic hydrophilicity the starch makes the paper surface more prone to adsorb water. For some paper grades it is sufficient to surface size with only starch but in most cases starch in combination with polymer particles are used. The surface sizing starch and the paper fiber are usually negatively charged[36] but also cationic starch or enzymatically degraded starch that is almost uncharged are used in some paper mills. Different starches are used for different grades. For printing and writing grades oxidized potato or maize starch are used. For packaging grades cheaper, native wheat and corn starches, enzymatically degraded on site, are the most common starches employed.

5.2.1. Starch for surface sizing application

Starch is a biopolymer with glucose as the repeating unit connected through α (1→4) glycosidic bonds. The polyanhydroglucose chain can form two types of polymers: amylose and amylopectin. The amylose chains are linear and relatively short while the amylopectin is highly branched and of high molecular weight. Different types of native starch have different proportions of amylopectin and amylose in the granules. The composition of regular potato starch is typically 20 wt% amylose and 80 wt% amylopectin.[37] In contrast, waxy starch contains only amylopectin. Native starch has a very high average molecular weight and gives rise to high viscosity when dissolved in water. Therefore the starch used for surface sizing is degraded prior use in order to decrease the molecular weight, which leads to reduced solution viscosity. The degradation is done by either oxidative, enzymatic or thermomechanical treatment and depending on degradation method the starch will have somewhat different molecular weight distribution and charge.

In this research work oxidized starch was employed where for which the oxidation is typically done with sodium hypochlorite (NaClO). The process leads to a depolymerization of the starch and at the same time oxidation of hydroxyl groups on the anhydroglucose rings generating carboxylic groups.[38] Thus, oxidized starch will have lower molecular weight and carry an anionic charge, which will be pH dependent. The charge density depends on the amount of NaClO added, and typical

values of degree of substitution (carboxyl groups) are 0.03-0.05 for oxidized potato starch. The structure of oxidized starch is schematically shown in Figure 5.

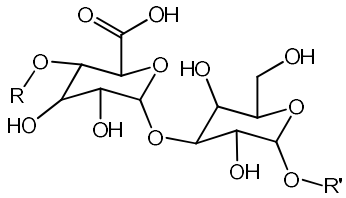

Figure 5. *Structure of oxidized starch.*

The starch mainly used in this research work is an oxidized regular potato starch. For some of the studies the influence of amylopectin and amylose was investigated and then a second starch type, an oxidized waxy potato starch was also included in the studies.

5.2.2. Size and charge

The SEC method is a chromatographic technique that separates the starch sample with respect of chain lengths, where the longer polymer chains are eluted first. The combination of Refractive Index, RI, and Multiple Angle Light Scattering detectors gives the absolute molecular weight and the molecular weight distribution of the analyzed sample. The results from the SEC analysis are listed in Table 2. The waxy starch is less degraded compared to the regular starch, giving the waxy starch a higher molecular weight and also a somewhat lower anionicity. The polydispersity index, Mw/Mn, for regular starch is higher compared to the waxy starch. This is due to the amylose part of the regular starch since amylose chains have low molecular weight compared to amylopectin. The polydispersity for the waxy starch is due to the natural origin of the polymer and also due to the oxidation process. The RI response for the oxidized starch is in accordance with previous studies where SEC was used for determining the molecular weight distributions of oxidized starch.[39]

Table 2.
Starch properties.

Sample	Mn (g/mol)	Mw (g/mol)	Mw/Mn	Colloidal charge (μeq/g)	R_G (nm)*
Regular starch	202,000	870,000	4.3	-176	7
Waxy starch	1,380,000	3,090,000	2.3	-127	7

*R_G from SAXS.

From SAXS measurements the radius of gyration was determined to 7 nm for both the regular and the waxy starch. Since both starch types were found to have the same radius of gyration it was concluded that only the amylopectin was detected by SAXS.

The colloidal charge for the two starches in solution was determined by colloidal charge titration where the anionic starches were titrated with a cationic polymer with a known charge density. The colloidal charge was determined to -176 μeq/g and -127 μeq/g for the regular and the waxy starch respectively. The difference in charge is due to difference in degree of oxidation as discussed above for the molecular weights. Since the starch has very low scattering intensity the ζ potential could not be determined.

5.3. CHARACTERIZATION OF THE TEST PAPER TYPES

Two types of model papers were used, one recycled liner grade and one fine paper grade. Recycled liner is an unbleached paper board type that consists of 100 % recycled fibers. This results in a very diverse paper composition that can vary from time to time. The liner is not internally sized but have some hydrophobic character due to residues of lignin and extractives in the paper. The fine paper grade was from a pilot machine and the composition is therefore well-defined. The fine paper was internally sized. This is necessary in order for the thin, hydrophilic paper sheet not to disintegrate during the surface sizing procedure.

5.3.1. Colloidal charge of fiber slurries

The colloidal charge was determined by colloidal charge titration using a particle charge detector, PCD, on a slurry of disintegrated paper. The anionic charge of the liner grade was determined by PCD to be -10 μeq/g. This is lower than has been reported in the literature for pulp slurries[36] but reasonable considering the fact that the liner is constituted of recycled fibers and that the fibers loose some charge during repulping. The anionic charge of the fine paper grade was determined to be -5 μeq/g which is also lower than expected. However, the cationic starch and the filler, GCC, might contribute to this low colloidal charge. The anionic charge in the fine paper is due to oxidation of the hydroxyl groups on the cellulose ring during pulping. For the recycled liner grade the anionic charge might originate from residues of lignin (oxidized), extractables (fatty acids, resin acids) as well as from processing conditions rendering carboxylic groups on the cellulose.

5.3.2. X-ray photoelectron spectroscopy, XPS

The chemical composition of the paper sheet surface as determined by XPS is summarized below (Table 3). As comparison the composition of filter paper made of pure cellulose is included in the table. The fine paper has similar elementary composition as the pure cellulose filter paper except from the calcium content that comes from the calcium carbonate used as filler. The chemical composition of the test liner is somewhat different and that is due to the residual content of lignin, fatty acid, resins and other compounds.

Table 3.
Chemical composition of the two test paper grades. Also included in the table is the chemical composition for a filter paper.

Paper type	Carbon	Oxygen	Calcium	Other
Filter paper	54.7	45.3		
Fine paper	55.7	41.0	3.3	
Liner	66.1	32.3	0.3	1.3

The anionic charge of the fibers determined by the PCD titrations originates only from carboxylic groups since the XPS analyses did not show any sulphur content which rules out the possibility of anionic sulfonate groups contributing to the anionic charge.

5.3.3. Permeability of the paper

In Table 4 the roughness and porosity properties of the liner and the fine paper grade are listed. The fine paper is determined to have larger porosity compared to the liner grade which might seem contradictory since the density of the fine paper is higher. However, what is not captured in this type of porosity measurement using air flow is the impact of the paper thickness. The liner grade has more than twice the thickness compared to the fine paper and if the porosity is normalized by the thickness the porosity for the fine paper grade would be around three times lower than the liner grade. The roughness measurements show that the liner is around five times more rough than the fine paper grade.

Table 4.
Properties of the test papers used in this study.

Paper type	Porosity (ml/min)	Roughness (ml/min)	Grammage (g/m^2)	Thickness (µm)	Density (g/cm^3)
Fine paper	390	370	80	103	775
Liner	350	2300	140	214	644

5.3.4. Scanning electron microscopy, SEM

The SEM images reveal a very open fiber structure with a pore size above 1 µm for both the fine paper and the liner as seen in Figure 6 a, b. The fibers in the fine paper show a defined shape and the more flexible fibers in virgin pulp give a more oriented fiber surface. The recycled fibers in the liner are more damaged and less flexible. It can also been seen that the liner contains more undefined material between the fibers.

The higher magnification SEM image of the fine paper surface, Figure 6 c), clearly show the filler particles (GCC) that can be seen as small irregular bright particles. The high magnification pictures also reveal a much more structured fiber surface for the fine paper that is not seen for the liner, see Figure 6 c) and d).

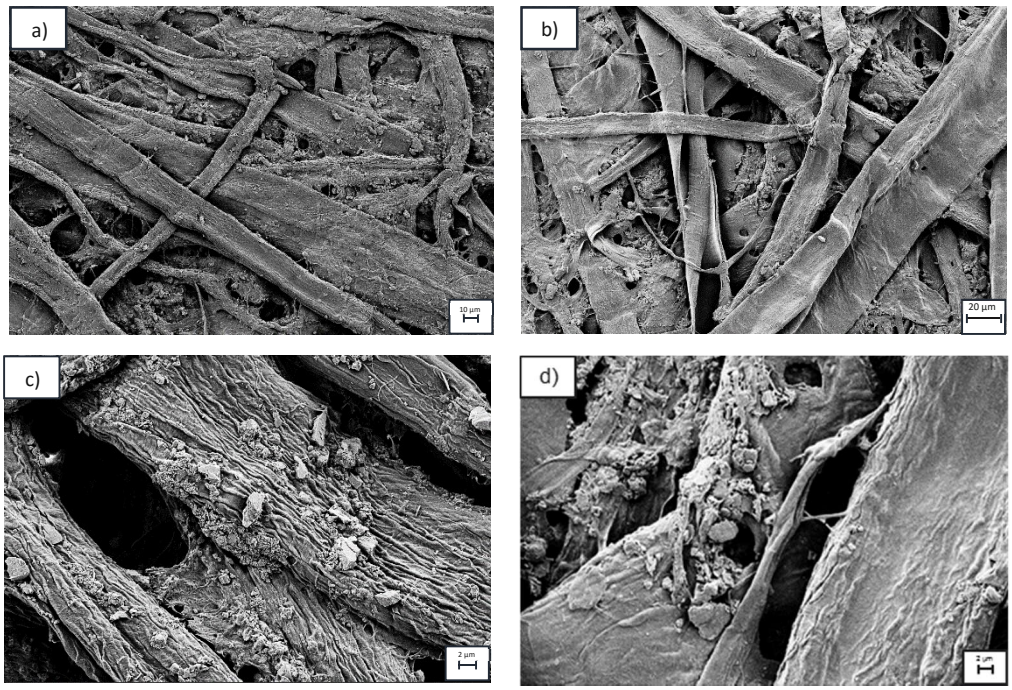

Figure 6. *SEM images of a) fine paper, b) liner, c) fine paper, larger magnification showing the GCC particles and a structured fiber surface, and d) liner, larger magnification showing a smooth fiber surface.*

6. RESULTS AND DISCUSSION

6.1. Colloidal behavior of sizing nanoparticles prior to the application

The first step in the surface sizing process is the mixing of the particle suspension with the starch solution. By mixing charged nanoparticles with a polyelectrolyte interactions occur depending on the nature of the particles and the polyelectrolyte. As described earlier, the colloidal behavior is expected to influence the performance of the surface sizing process. Therefore a study of the three particles types SP+, SPA and SP- in presence of an oxidized starch in solution was performed.

6.1.1. Colloidal behavior of SP+, SPA and SP-

The colloidal behavior of the combination of the particles and starch was studied by monitoring the change in turbidity of the particle suspension when starch was added. The particle concentration was 0.1 wt%, which is a typical particle concentration in surface sizing. The starch was added in small aliquots of 20 µl to a 2 ml particle suspension and after vigorous shaking the turbidity was measured. For the slightly anionic SPA and the highly anionic SP- the addition of starch did only marginally affect the turbidity. A small decrease in turbidity was seen, which can be attributed to the minor dilution of the particles upon addition of the starch solution. The cationic particles, SP+, on the other hand showed an interesting and very different behavior (Figure 7). Already the very first aliquot of starch gave rise to an increase in turbidity due to formation of aggregates in the system. The fact that the aggregation took place even at very low starch to particle ratio shows that the stability of the cationic particle suspension was strongly affected by the oppositely charged polyelectrolyte. The turbidity increased further with increasing addition of starch. This is in accordance with previous studies of similar systems.[40-44] The turbidity increased to a maximum at a specific starch concentration, corresponding to 1:1 in charge ratio for the cationic particles and the starch. Further addition of starch partially restored the stability of the dispersion, as seen by a decrease in turbidity above this charge ratio. However, the turbidity did not return to the initial value for the primary cationic particles, indicating that even in the presence of an excess of starch, there are still aggregates in the suspension. At a starch concentration of 8 wt%, corresponding to the application conditions, the turbidity of the combination of cationic particles and starch is still higher than the initial value, 0.18 vs. 0.06 in turbidity, giving further

support for the presence of aggregates even when starch is in large excess. Long term studies have shown that these aggregates are stable for several weeks of storage.

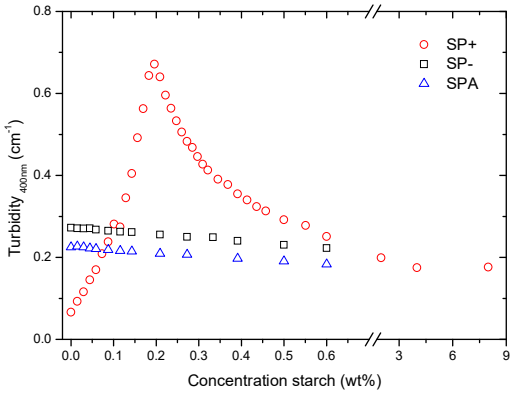

Figure 7. *Turbidity as a function of starch concentration for SP+, SP- and SPA. Note the break in the x-scale.*

In previous studies the addition order[45-47] as well as the mixing rate[48, 49] have been found to have a critical impact on the aggregate formation. Both different addition orders and different stirring rates were therefore tested. In the present system it was found that neither the addition order nor the stirring rate were decisive for the outcome. For the combination of SP+ particles and starch it was found that the same aggregation behavior was achieved irrespective of how the SP+ particles and starch were mixed. Also for the SPA and SP- particles there was no impact on turbidity with the addition order or stirring rate. No turbidity change was induced by the addition of starch.

The amphoteric SPA particles carry cationic charges but are net anionic due to oxidation. From this turbidity study it can be concluded that it is the net charge that will determine if there is an interaction between the particles and the starch within the conditions used in this experimental setup.

The nature of the formed aggregates of SP+ and starch was subject to further studies exploring the size, charge and internal structure of the aggregates. The aggregation mechanism and the impact of the starch properties, as well as the kinetics of the aggregation, were investigated.

6.1.2. SP+ and starch aggregate characterization

The maximum in turbidity was found to be at a starch to particle ratio corresponding to 1:1 in charge ratio determined by PCD titration of the SP+ particles with the starch as titrant. For different starch to particle ratios also the particle size and the ζ potential were measured. Both the radius of hydration and the radius of gyration of the aggregates were determined. When the turbidity, the particle size and the ζ potential are plotted versus starch to particle charge ratio, as was made in Figure 8, an interesting feature is revealed; the maximum in turbidity, as well as the maximum in particle size, coincides with the ratio where the ζ potential reaches zero. This demonstrates that when starch is added to the SP+ particles it adsorbs on the SP+ particle surface due to electrostatic interactions and at the same time it decreases the cationic charge of the complex, which destabilizes the system and causes aggregation. The magnitude of aggregation increases with increasing starch concentration up to charge neutralization. Above the 1:1 in charge ratio the particle size, as well as the turbidity, decreases with further starch addition, which can be seen as a restabilization of the system. At this point the ζ potential is negative, which demonstrates that starch is still adsorbed beyond the neutralization point, probably due to other attraction forces like van der Waals interactions. The overall anionic charge of the complex contributes to the restabilization of the system.

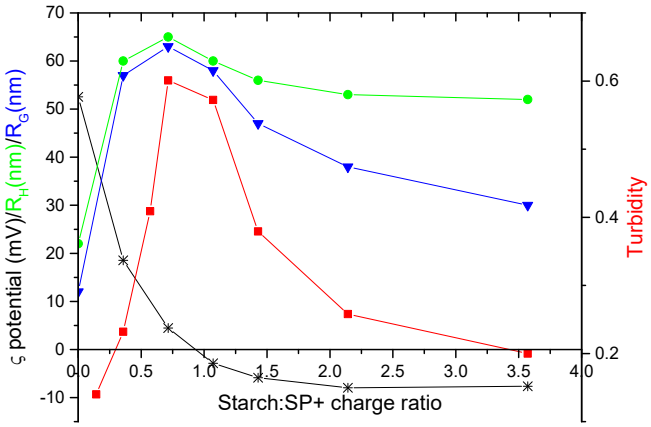

Figure 8. *Plot of turbidity, particle size, and ζ potential vs. starch to particle charge ratio.*

The examination of the ratio of R_H to R_G showed that during the restabilization phase, i.e. at higher starch to particle charge ratios, the R_G/R_H ratio decreases. This could be due to the change of the structure of the aggregates from a hard sphere-like system towards a gel-like structure[50] and this could also be the reason why R_H levels out before the turbidity does.

Several authors have reported that on addition of a polyelectrolyte to a suspension of oppositely charged colloidal particles there is a minimum in stability at a certain amount of added polyelectrolyte.[40, 41, 44, 51, 52] This is in accordance with the results from this study, with the maximum in turbidity corresponding to the most destabilized state.

The effect of particle concentration was investigated using different SP+ concentrations for the starch titrations and it was concluded that the particle concentration did not affect the aggregate size at maximum aggregation.

The starch type here labeled regular starch, consists of the linear, shorter amylose molecules and the branched, longer amylopectin molecules at a mass ratio of 20:80. Size exclusion chromatography, SEC, was employed in order to investigate the possibility of preferential adsorption of one of these components during the aggregation process. For the starch-particle combinations where charged neutralization was not yet obtained, i.e. at low starch to particle ratio, the analysis showed that the fraction corresponding to higher molecular weights, i.e. the amylopectin, had disappeared while a significant part of the lower molecular weight fraction of the starch, i.e. the amylose, remained in solution even though the starch was in deficit. Thus, it seems that only the amylopectin fraction of the regular starch took part in the aggregation with the oppositely charged particles. To confirm this hypothesis a second starch type was introduced in the studies, the waxy starch that contains only amylopectin. The waxy starch showed the same turbidity behavior as the regular starch and the depletion of the high molecular weight part of the waxy starch obtained from the SEC analysis confirmed that it is mainly the amylopectin fraction in regular starch that participates in the aggregation, as seen in Figure 9.

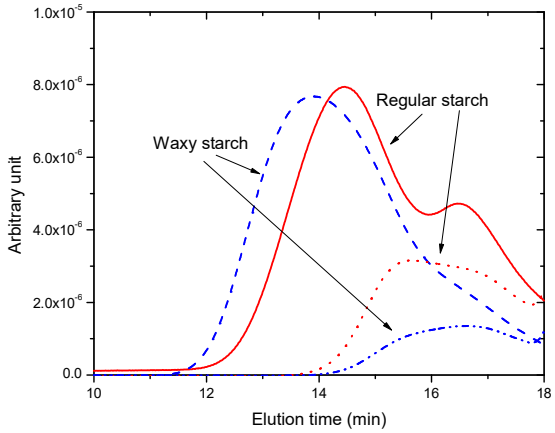

Figure 9. *RI chromatograms for regular and waxy starch (solid lines) and for the starch remaining in solution after aggregation with SP+ particles, using a starch to particle charge ratio of 1:1 (dashed lines).*

The observation that the amylopectin fraction of the starch is responsible for the aggregation is interesting and can help explaining why the formed aggregates are stable despite their low charge density. The highly branched and negatively charged amylopectin molecules that cover the positively charged particles are likely to give good steric stabilization. This is a proper example of so-called electrosteric repulsion.[27]

The inner structure of the aggregates formed from combinations of starch and SP+ particles was characterized by SAXS within the charge ratio interval 0.19:1 to 3.8:1. The SAXS data were plotted in a log-log diagram of $I(q)$ *vs.* q and were fitted with the unified equation (4). A structural level is reflected as a kink and a linear region in the plot, and in Figure 10 two structural levels can be seen. At the lowest q values a plateau of is found and the R_{G1} parameter, i.e. the size, can be determined. The slope of the decay that follows the plateau with increasing q gives the P_1, which describes the fractal dimension of the aggregates. At higher q another plateau is found and here R_{G2} is determined and followed by a decay where the slope gives P_2. R_{G1}, P_1, R_{G2} and P_2 were evaluated for the various starch to particle charge ratios studied. R_{G1} was found to increase with increasing starch to particle charge ratio up to charge neutralization, demonstrating that the starch chains are adsorbing onto the surface of the primary particles and not only on the outer surface of the aggregates. For the

primary particles P_1 was 3.8, i.e. the particles have a rough fractal surface. This fractality was preserved for the aggregates up to charge neutralization. With the starch in excess P_1 was lower and this could be due to denser packing of the starch chains on the surface, which is also seen by a minor decrease in R_{G1} at this point. The SEC analysis showed that it is mainly the amylopectin fraction of the starch that participates in the aggregation, which is in accordance with the SAXS data. The values of R_{G2} and P_2 for the second structural level are in good agreement with the corresponding values for the starch, also showing that the conformation of the amylopectin chains is preserved in the aggregates.

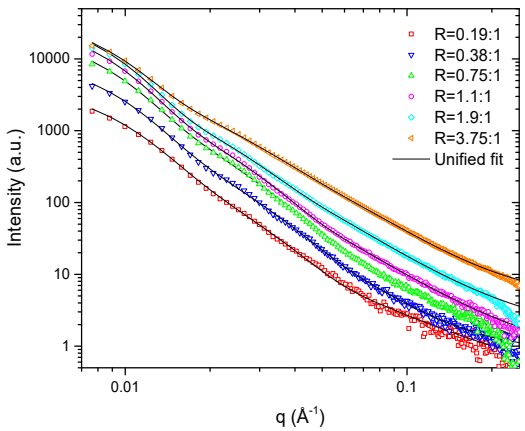

Figure 10. *Log-log plot of SAXS data for a combination of starch and SP+ particles at different charge ratios (R). Lines are unified fits to the data.*

Above the 1:1 in charge ratio a further addition of starch did not significantly affect the internal structure of the aggregates, i.e. the starch covered SP+ particles remain intact even though the overall aggregate carried a net anionic charge. As can be seen from the turbidity measurements and the changes in R_G/R_H ratio, the overall aggregate size and structure are affected when an excess of starch, in terms of charge ratio, is added to the SP+ particles. This is probably due to additional adsorption of starch on the more accessible, outer surface of the aggregates, giving rise to the anionic charge that induces repulsion between the aggregates, which give a gel-like structure and a decrease in size.

6.2. Formation and relaxation kinetics of starch-particle complexes

The understanding of the formation path and the stability of the formed aggregates are of interest if the aggregates are important for the surface sizing efficiency since this can create an opportunity to tailor the aggregates for enhancing surface sizing performance.

6.2.1. Aggregate formation

The aggregate formation when the anionic starch is added to cationic particles was studied with DLS. The SP+ particles were found to have too high diffusion rate and thereby too fast collision rate to be monitored with DLS. Cationic amidine particles with a radius of 110 nm were therefore used as a model system since larger particles have slower diffusion, making monitoring of the aggregate formation possible. To ensure that the model system was similar to the SP+ particles a charge titration of the amidine particles with starch was performed and it was found that the charge neutralization and the shift in ζ potential from positive to negative was comparable. It was therefore concluded that this model system could be used. From this DLS study the stability ratio, W, was determined, shown in Figure 11. The stability ratio is defined as $W=k_{fast}/k$, where k_{fast} is the aggregate rate coefficient at maximum rate of aggregation and k is the aggregate coefficient in the studied conditions. The inverse stability ratio represents the likelihood of obtaining a dimer upon collision between two particles. For a totally destabilized system the stability ratio is around 1. In the system studied here it was found that the minimum in W did not reach 1 meaning that there is a stabilizing mechanism also when the system is charge neutral. This confirms that there is steric stabilization from the adsorbed branched, high molecular weight amylopectin chains also at the charge neutralization point.

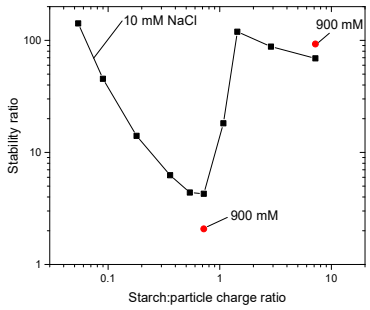

Figure 11. *Stability ratio as a function of starch to particle charge ratio. 10 mM NaCl background was used (black full squares). Two point with 900 mM NaCl background are also presented (red full circles).*

6.2.2. Aggregate relaxation

The change in turbidity with time was monitored at different starch to particle charge ratios, whereby the *relaxation* rates could be extracted. This was done at different particle concentrations and different temperatures as well as with both regular and waxy starch.

When starch was added to the cationic particles the initial turbidity measured right after mixing was found to be higher than the equilibrated value. The magnitude of the difference in turbidity with time was found to be most pronounced around the maximum in turbidity and it was also found that the waxy starch gave rise to a larger difference between the initial and the equilibrated turbidity compared to the turbidity increase for with the regular starch. A concentration dependence was also found by comparing the turbidity curves for two particle concentrations; 0.1 wt% and 0.05 wt% in Figure 12 from which two main differences can be distinguished. First, the magnitude of the turbidity increase is more pronounced for the higher particle concentration. This could be expected as more particles are present in the suspension, which means that more aggregation can take place for the same starch to particle ratio. The second effect is that the initial kinetic contribution to the turbidity increase is higher for the particle concentration of 0.1 wt% compared to that of 0.05 wt%, as the difference between the initial and final turbidity values are more pronounced at the higher particle concentration. At a higher particle concentration the collision rate, r_c, is higher and this could lead to non-equilibrium flocculation that can take place to a larger extent.[53, 54] Initially the starch chains have the possibility to interact with more than one particle surface, forming bridges between the particles. Then rearrangement of the starch chains occurs giving a starch patch adsorbed on the particle surface which leads to a denser structure and a decrease in turbidity with time. These results also explains why relaxation cannot be seen by dynamic light scattering, where the aggregate formation was captured. The very dilute particle and starch system mainly allowed doublets to form and therefore bridging flocculation was unlikely to occur.

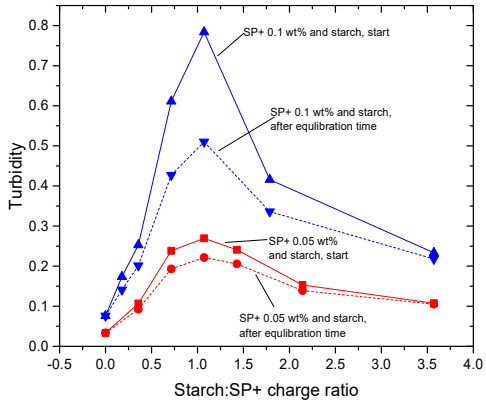

Figure 12. *Turbidity curves for two different SP+ particle concentrations, 0.05 wt% and 0.1 wt%. The highest SP+ particle concentration gives the highest turbidity increase. The initial turbidity increase is more pronounced for the highest particle concentration.*

The turbidity experiments were performed at room temperature, but in reality surface sizing is usually carried out at elevated temperature in order to avoid retrogradation of the starch. Experiments performed also at 40 °C and 60 °C showed that the particle suspension and the starch solution were found not to be affected by the elevated temperatures but when they were combined the turbidity had a temperature dependence when it comes to relaxation. The overall colloidal behavior of the SP+ and starch was preserved at elevated temperature, i.e. the turbidity curves were similar and the maximum was at the same starch to particle charge ratio, but the magnitude of the turbidity differed. There was a decrease in the turbidity maximum with increasing temperature. When comparing the initial turbidity curve performed at 60 °C and the curve for the equilibrated values at room temperature a good agreement of the points was found. This is reasonable since the system is more dynamic at higher temperatures which leads to a faster reorganization of the starch chains from bridging to patches on the particle surfaces.

These findings show that the relaxation rate after aggregate formation can be accelerated by increased temperature, but in the end the remaining, stable, aggregates will be the same. This result can also be used to tune the state of aggregation by using time or temperature as a controlling factor.

By monitoring the variation of turbidity with time the kinetic pattern could be extracted; the turbidity value decreased with time until a plateau was achieved, i.e.

when equilibrium was reached. Moreover, the decrease was more pronounced at higher initial turbidity. Both the regular and the waxy starch were monitored in combination with the SP+ particles and it was found that the relaxation behavior was the same but the time interval for reaching the plateau was longer for the waxy starch. The relaxation behavior of the turbidity with time was evaluated by fitting the normalized experimental data with the Kohlrausch-Williams-Watts (KWW) relaxation function. This function is used to describe various types of relaxation data and it is often used as an universal model for studying various physical and chemical processes.[55]

The KWW equation is expressed as $y(t) = e^{\left(-\frac{t}{\tau}\right)^{\beta}}$ (1)

where *y(t)* is the relaxation function expressing the kinetics for the transformation of non-equilibrium to equilibrium state,[56] τ is the mean relaxation time, and β the relaxation distribution parameter, which describes how the relaxation deviates from exponential behavior.[56, 57] The parameter τ can be seen as a description of the range of relaxation times where most of the relaxation processes take place.[58] The β value can vary between 0 and 1 and when β=1 the KWW relaxation function becomes an exponential expression. The β parameter can also be seen as a measure of the heterogeneity of the relaxation process. If β is close to 1, the relaxation process is regarded as homogeneous.[59]

By examining the parameters obtained from the KWW equation it was found that the relaxation time, τ, for the aggregates was the same irrespective of the position along the turbidity curve vs. starch concentration. In other words, irrespective of the particle to starch ratio and of the net charge of the complex (as determined with ζ potential), the time for going from an initial aggregation state to the relaxed equilibrated state, where the starch chains have had sufficient time to rearrange on the particle surface, was the same. Interestingly, a difference between the starch types could be seen. This is shown Figure 13 where one turbidity curve for SP+ and regular starch and one turbidity curve for SP+ and waxy starch are plotted versus time together with the KWW fittings. On average, the relaxation time for the regular starch was around 1400 s and for the waxy starch around 4800 s. The waxy starch that has a higher molecular weight thus takes much longer time for rearrangement of the starch chains on the particle surface. The higher anionic charge for the regular starch gives a stronger surface attraction.[60] This might also contribute to the difference in relaxation time between the regular and the waxy starch along with the difference in molecular weight.

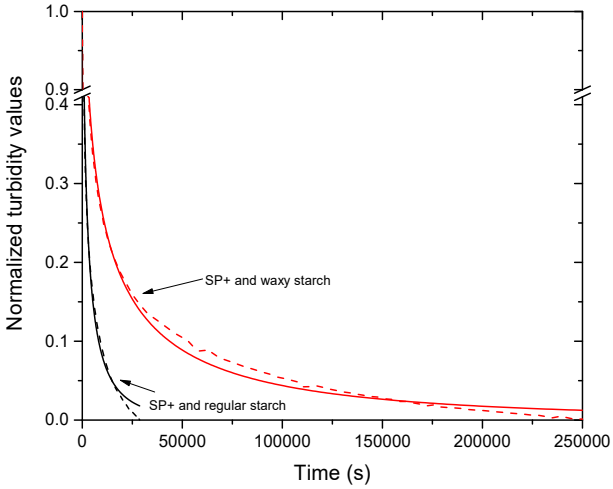

Figure 13. *Normalized turbidity data. For simplicity one curve (dashed lines) for each starch type is shown in the figure together with the fitting of the KWW function (solid lines). Note the break in the curve.*

A SAXS study was performed in order to investigate whether the inner structure of the formed aggregates was affected by the relaxation process evidenced by the turbidity measurements. The cationic particles were titrated with the regular starch. The time for sample preparation and the measuring time did not allow to capture the aggregation as early as in the turbidity measurements. The first time point is approximately three minutes after mixing. The scattering intensity for each sample was monitored for one hour. No change in intensity over time could be seen for the different starch to particles ratios.

6.2.3. Aggregate formation and relaxation with waxy starch

In the aggregate relaxation study it was shown that the waxy starch has slower relaxation and the hypothesis was that also the formation of aggregates might be slower with the waxy starch. To test this hypothesis an experiment was performed using a MALS instrument to follow the aggregate *formation,* as well as the subsequent *relaxation,* for SP+ particles in combination with the waxy starch. The aggregate formation and the relaxation kinetics were monitored for the starch to particle charge ratio corresponding to maximum turbidity, i.e. close to neutrality. Figure 14 shows the results from these measurements with the size of the aggregates plotted against time. The aggregate *formation* gave rise to a rapid increase in size up

to a plateau around 80 nm. With time, the size of the formed aggregates started to decrease due to relaxation of the starch chains. The aggregate size levels out after approximately 500 minutes. This is in agreement with the turbidity measurements, where it was found that the turbidity reached a plateau after similar equilibration time. The increased size of the aggregates after long time compared to the primary particles showed that also after relaxation there were still aggregates in the system.

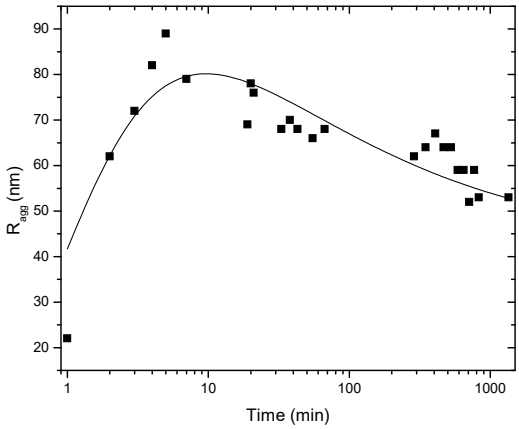

Figure 14. *Aggregate formation and subsequent relaxation of SP+ particles in combination with waxy starch. The line is a guide for the eye.*

6.3. Mechanism of aggregation

Possible mechanisms for polyelectrolyte-induced aggregation of colloidal particles of opposite charge are extensively discussed in the literature and two different mechanisms are in focus; bridging and patchwise flocculation. Bridging flocculation can occur when one part of the polymer chain is adsorbed on two or more particle surfaces at the same time, forming a bridge between the particles.[61] This aggregation mechanism requires concentrated suspensions and high molecular weight polymers.[51] The other important aggregation mechanism that is discussed in the literature is patchwise flocculation[41, 42, 62-67] where it is stipulated that the charged polymer chain adsorbs onto the particle surface due to electrostatic attraction. This leads to a local charge reversal on the part of the particle surface that has been covered; thus, the particle surface now contains patches of opposite charge. This may lead to electrostatic attraction between covered patches on one particle and uncovered patches on another particle. In the SP+ and starch aggregated system we are suggesting that both are occurring, but at different time scales.

From turbidity measurements it was shown that aggregation started already at a low ratio between the anionic starch and the positively charged particles. As demonstrated by the SEC and SAXS experiments it is mainly the amylopectin molecules that are adsorbed on the positively charged particle surfaces causing the aggregation.

By using relatively high particle and PE concentration, comparable to the industrial application, the time for particle collision is, according to Smoluchowski theory,[68] only around 3 ms. This means that the adsorbed polymer chain will not have sufficient time for rearranging on the particle surface before the particle collides with another particle and the particles will thereby collide with the polymer chains attached on the surface in a non-equilibrated conformation. At this state it is possible for the starch chains to interact with more than one particle through bridge flocculation. This is in the literature referred to as non-equilibrium flocculation. In the relaxation study this was seen for the SP+ particles and starch system as a decrease in turbidity with time. There was also a molecular weight dependence on the relaxation time. The waxy starch, which has three times higher Mw than the regular starch, also has three times longer relaxation time. This observation supports the hypothesis that there is an initial aggregation state where bridging flocculation occurs since this aggregation mechanism is strongly governed by the molecular weight of the polymer.

With time, rearrangement of the starch chain occurs resulting in starch patches adsorbed on the particle surface and the aggregation mechanism is then moving towards patchwise aggregation,[69, 70] which leads to a decrease in turbidity.

For rapid formation of the aggregates a lower molecular weight PE is beneficial, but for the preservation of the maximum in aggregation a higher molecular weight PE is desirable. The molecular weight of the starch can thus be a key to control the aggregation.

After the equilibration time, which is when the adsorbed starch chains have reached their equilibrated conformation, the turbidity for the cationic particles in combination with the regular starch was comparable to the turbidity for the cationic particles in combination with the waxy starch. Thus, at equilibrium the turbidity is similar for both starch types despite the fact that the waxy starch has three times higher molecular weight than the regular starch. This supports the hypothesis of patchwise aggregation of the SP+ particles in combination with the starch. A schematic illustration of the aggregation mechanism after equilibration is shown in Figure 15.

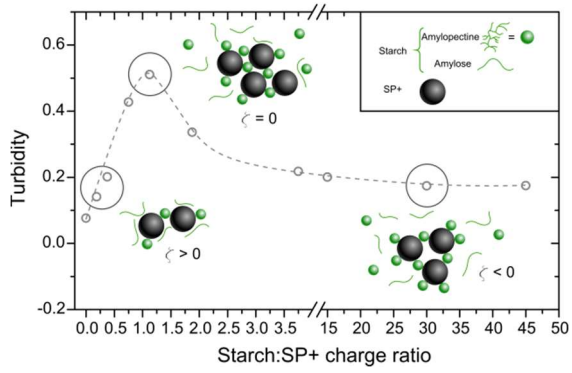

Figure 15. *Tentative mechanism for aggregation of regular starch, which is negatively charged and consists of a mixture of amylose and amylopectin, and positively charged particles.*

6.4. Evaluation of the surface sizing performance

The three particle types used in this study are all representatives of what is used in the paper industry today. The surface sizing efficiency was evaluated by applying the hydrophobic particles in combination with starch on different test papers. The application was done with a size press laboratory equipment.

In the size press method the final step is the drying step. The drying temperature is important for two reasons; to remove the water and to elevate the temperature to allow the film formation. The particle size for SP+ is smaller than for the other particles and this smaller size gives an increased surface area compared to SPA and SP-. The surface area is important for the drying process. Larger particles with smaller surface area have poorer energy transfer capacity, which may influence the flexibility of the polymeric core. However, in this case the drying temperature was high enough to ensure that the energy transfer was sufficient for all three types of particles.

SEM pictures were taken on both untreated and surface sized paper to examine the impact of the surface sizing on the structure of the paper surface. In the pictures shown in Figure 16 a-d it can be seen that addition of starch leads to a somewhat denser surface structure. For the paper sheets that were surface sized with SP+, SPA and SP- no further densification could be seen and no other signs of the presence of the surface sizing particles could be established with this method.

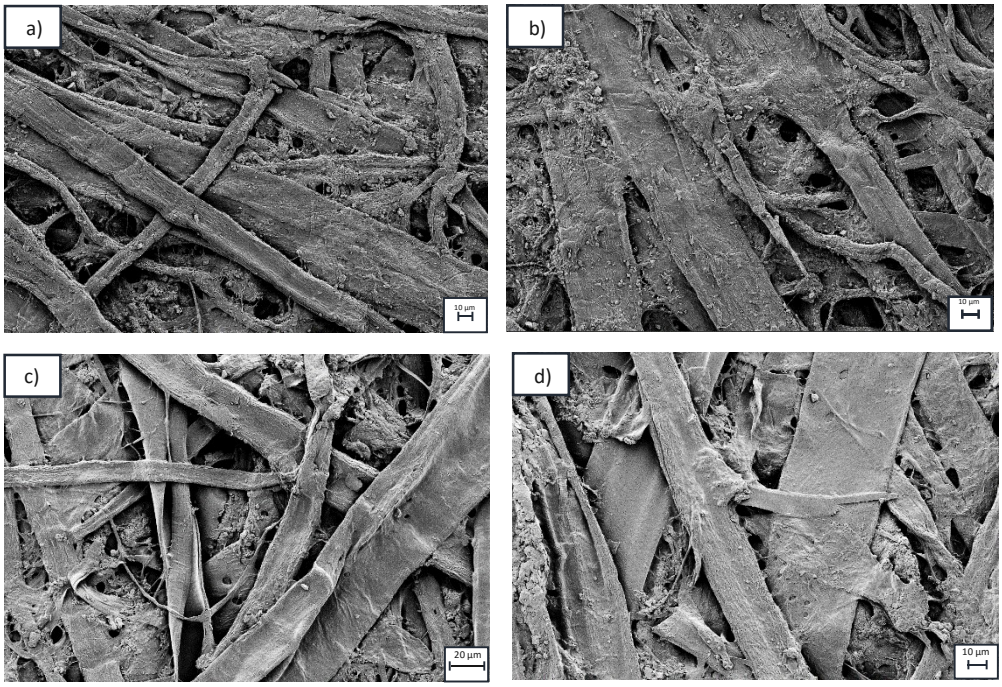

Figure 16. *SEM images of a) unsized fine paper, b) fine paper sized with starch, c) unsized liner, and d) liner sized with starch.*

The efficiency of the surface sizing was evaluated by measuring the decrease in water uptake due to the hydrophobization of the surface using the Cobb 60 method. The lower the water uptake the more efficient are the particles in making the surface water resistant.

Furthermore, the porosity and the surface roughness were examined for both untreated and surface sized paper sheets. It is known that these characteristics contribute to the rate of water uptake.

6.4.1. Permeability and roughness of the paper

When starch was applied on the paper surfaces the air permeability for both the liner grade and the fine paper grade decreased as a consequence of the starch on the paper surface filling the surface voids in the paper sheet.[11] No additional decrease in air permeability could be seen for neither the fine paper grade nor the liner grade when the mixture of starch and particles was applied. This is in line with the findings in previous studies of surface topography on similar systems, where it was concluded that surface sizing particles do not affect the surface structure.[71] The roughness of the fine paper grade was not affected by the starch application since untreated fine paper sheets already have a smooth surface due to the high filler content.[2] On the other hand, the roughness of the test liner was significantly decreased by the starch application, which is according to expectations since unsized liner has a high surface roughness compared to fine paper. However, no further increase in smoothness could be seen upon addition of the particles.

6.4.2. Water retention

The untreated fine paper grade had a water uptake of 81 $g.m^{-2}$. After exposition to starch at a concentration of 8 wt%, the water uptake increased to 107 $g.m^{-2}$, which is an indication of a more hydrophilic paper surface, as also observed in previous studies.[20, 71] The same effect was seen on the liner, where the untreated paper had a water uptake of 137 $g.m^{-2}$ which with starch increased to 154 $g.m^{-2}$.

Figure 17 shows the results from the Cobb 60 test for the three types of particles on the two paper grades using an increasing concentration of sizing particles while the starch concentration was kept constant at 8 wt%.

From this figure an interesting pattern emerges. The SP- and SPA particles had low sizing efficiency even at relatively high particle dosage. The SP+ particles behaved differently, however. The water uptake decreased rapidly when the particle dosage

was increased. The difference between the SP+ and the other two particle types is significant for both the fine paper and for the liner; however, the difference is much more pronounced for the former.

The results from this study show that even if the three particle types have the same hydrophobic core and thereby could be expected to contribute to the same extent to the hydrophobization when applied on the paper surface, there is a significant difference between them in terms of sizing performance. The main difference between the particle types is the colloidal charge of the stabilizer. It might seem obvious that particles with a cationic charge would have a better performance since the retention of the cationic particles on the negatively charged fibers in the paper can be expected to be superior to that of SPA and SP-. However, the particle suspensions are mixed with anionic starch, and the amount of particles used in the sizing formulation is very small compared to the amount of starch. Nevertheless, the results from the application study reveal interesting differences between the particle types regarding their efficiency in reducing water uptake.

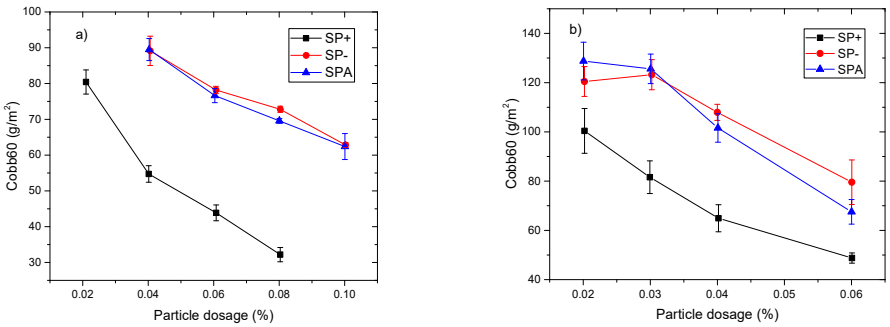

Figure 17. *Water retention as determined by the Cobb 60 test as a function of concentration of surface sizing particles together with a constant concentration of starch (8 wt%) for a) fine paper, b) liner.*

6.5. Correlating the colloidal behavior results with the surface sizing performance

In the study of the colloidal behavior of the SP+, SPA and SP- particles in combination with the anionic starch it was found that the cationic particles formed aggregates with the starch and a maximum in aggregation was found around 1:1 in

charge ratio between the starch and the particles. At starch concentrations above the 1:1 charge ratio the aggregates were decreasing in size and an overall restabilization of the system was observed as a decrease in turbidity. However, only partial restabilization seemed to occur and also at higher starch concentrations, corresponding to 8 wt% as used in surface sizing, stable aggregates were still present. It is conceivable that the aggregation of the SP+ particles with starch can explain the better performance of the SP+ particles compared to the SPA and SP- particles.

In the surface sizing method the starch concentration is held constant and different amounts of the particles are added to the starch solution giving different starch to particle ratios. Usually the starch to particle ratios are high compared to the 1:1 in charge ratio for starch and SP+ that was shown to give rise to a maximum in aggregation. To address this a size press trial was performed using different starch concentrations in combination with the particles to include both a low starch to particle ratio, i.e. 0.3 wt%, corresponding to maximum aggregation, and a high starch to particle ratio, i.e. 8 wt%. The hydrophobization efficiency for SP+ and SP- using either an 8 wt% or 0.3 wt% starch solution is shown in Figure 18. For the SP- particles, with which no aggregation was observed, the hydrophobization efficiency using a high or a low starch to particle ratio was similar. The SP+ particles showed superior hydrophobization efficiency when the starch to particle ratio corresponded to the maximum in turbidity showing that the colloidal behavior can have a significant influence on the surface sizing performance.

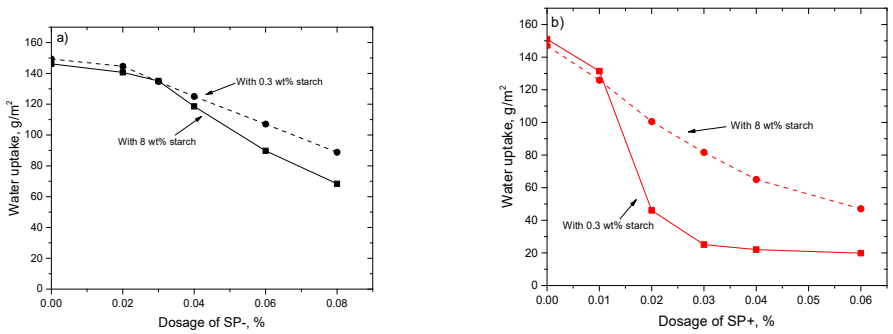

Figure 18. *Cobb 60 results at 0.3 and 8 wt% starch for SP- and SP+ particles. a) No impact of starch concentration on the SP- performance. b) A pronounced effect on SP+ was found at the starch concentration corresponding to a high aggregated state for the SP+ and starch.*

7. CONCLUSIONS

The three particle types that were used in this thesis work had the same hydrophobic polymer core but differed in the nature of the stabilizer. The SP+ particles were shown to interact with the anionic starch while the SPA and SP- particles behaviour was not influenced by the starch. The interactions between SP+ and the starch gave rise to aggregation that was found to be partially reversible and had a maximum around 1:1 in charge ratio between the starch and the SP+ particles. Even at high starch concentration the aggregates were stable in solution, as a result of the starch adsorbing on the particle surfaces. The SEC study showed that it was mainly the branched amylopectin component of the starch that gave rise to the aggregation with the cationic particles. The low molecular weight amylose remained in solution. This indicates a change of stabilization mechanism from electrostatic (for the primary particles) to electrosteric. The SAXS measurements showed that the amylopectin conformation was partly preserved. This confirms a patchwise aggregation mechanism where the starch chains locally change the surface charge from cationic to anionic and thereby facilitated aggregation between the locally negatively charged sites and the positively charged sites of bare surface of other particles.

The aggregation was found to have a time dependency. The initial turbidity was higher compared to that seen after equilibration. The difference in initial and final turbidity was largest around the maximum in turbidity and was also larger for the waxy starch compared to the regular starch. Fitting of experimental data using the KWW function revealed that the relaxation time was independent on the starch to particle ratio but a difference could be seen between the two starch types. The higher molecular weight waxy starch had a longer relaxation time. This implies that there is an initial aggregation state where polymer bridging occurs but with time, when the starch chains have had sufficient time to relax on the particle surface, this bridging effect is decreased and the aggregation mechanism is changed towards patchwise aggregation.

The surface sizing efficiency of the three particle types SP+, SPA and SP- was evaluated by the Cobb 60 method. It was found that the SP+ particles had the best performance for the two test paper grades, fine paper and liner, correlating with aggregate formation in presence of starch.

The SP+ particles are more aggregated at lower starch concentration compared to the 8 wt% usually employed in surface sizing. Therefore a study at 0.3 wt% starch was performed and the results showed that the performance of the SP+ particles was greatly improved by the lower starch to particle ratio while the performance of the SP- particles was not affected by the ratio between the two components.

8. FUTURE WORK

The study concerning the bulk behavior of the particle/starch systems will be continued with emphasis on the effect of salt both on aggregation and on surface sizing.

The particles and the formed aggregates will be investigated with AFM.

By using fluorescent labelled particles in the surface sizing trials the distribution and penetration will be studied using microscope methods.

ToF-SIMS analyses are on-going in order to get chemical information about the surface sized paper sheets. These results will be correlated to sizing performance and to the results from the planned fluorescent studies.

Film formation and film properties of the particles as a function of starch addition and temperature will be investigated with AFM, ToF-SIMS and by contact angle measurements.

ACKNOWLEDGEMENT

The Swedish Research Council is acknowledged for financial support.

The VINN Excellence center SuMo Biomaterials is acknowledged for economic and scientific support.

The opportunity to go to MAX IV Laboratory for SAXS beam time is acknowledged.

I would also like to thank:

My supervisor Romain Bordes for your engagement in my project, for interesting discussions and guidance in my project. For always having time for last minute reviews!

My supervisor Professor Krister Holmberg, I'm so grateful for your support and advice!

My steering group committee members, Heidi Fagerholm, Anneli Lepo, Maria Wallgren and Jonas Engström for being so supportive and engaged in the project.

My former supervisor Professor Mats Andersson for initiating the project.

My co-authors Professor Aleksandar Matic and Gregor Trefalt.

My examiner Professor Anders Palmqvist.

Tuan Phan Xuan for helping me with the MALS and SAXS measurements and for your contributions to the papers.

Ann Jakobsson for all administrative help and for nice coffee room chats.

Anne Wendel for performing the XPS analyses.

Anders Mårtensson for helping me with the SEM analysis.

Annika Altskär for helping me with the TEM analysis.

Linda Härdelin, for having the SEC-MALS/RI system in a good shape so I just could jump in with my samples!

Krzysztof Kolman for the discussions about DLS and KWW theory.

My roommate Negin Yaghini for all nice discussions about work and life.

Sanna Björkegren for being such a great travel company!

All former and present colleagues at TYK, KCK and floor 8 for creating such a great atmosphere.

My colleagues at Kemira Kungälv for all the valuable help with lab equipment and for helping me with questions about paper chemistry. Special thanks to Kerstin Malmborg for her excellent work with the size press trials.

Michael Persson, Per Restorp and John Sandström at AkzoNobel for initiating this project and special thanks to Per for the help and guidance in the beginning of the project.

My former colleagues at AkzoNobel PPC, special thanks to Daniel Persson for always being up for discussions. Of course also special thanks to Olle Hidestål for being such a great roommate!

To my family and friends, thanks for all your support. Special thanks to my parents for always supporting me in whatever I do! Mum, thanks for your support and invaluable help with Matilda!

To Robert, for always encouraging me to go my own way and do what I want. And for your endless support (and patience) when I do! I love you!

To the lights of my life; Matilda and Harry. For the overwhelmingly love and energy you give me!

REFERENCES

1. P. Bajpai, *Paper and Paperboard Industry*, Elsevier, USA, 2015.
2. B.-U. Cho and G. Garnier, *TAPPI Journal*, 2000, **83**, 1-18.
3. J. M. Gess, in *The Sizing of Paper*, ed. J. M. R. Jerome M. Gess, TAPPI Press, Atlanta, Third Edition edn., 2005, ch. 1, pp. 1-7.
4. N. Yang and Y. Deng, *Journal of Applied Polymer Science*, 2000, **77**, 2067-2073.
5. H. O. B. T. Lindström, *Nordic Pulp and Paper Research Journal*, 1986, **1**, 34-42.
6. M. A. Hubbe, *BioResources*, 2014, **9**, 5782-5783.
7. G. Garnier, J. Wright, L. Godbout and L. Yu, *Colloids and Surfaces A: Physicochemical and Engineering Aspects*, 1998, **145**, 153-165.
8. S. Iwasa, presented in part at the Scientific & Technical Advances in the Internal & Surface Sizing of Paper & Board, Prague, 12-13 December 2001, 2001.
9. J. Anderson, in *Surface Application of Paper Chemicals*, ed. I. T. J. Brander, Springer Science & Business Media, London, 1997, pp. 138-155.
10. B. W. Ranson, *Pulp and Paper*, 2004, **78**, 50-54.
11. C. P. Klass, *Pulp and Paper Manufacture* 1991, **17**, 306-322.
12. R. T. Gray and D. S. Rende, in *The Sizing of Paper*, ed. J. M. R. Jerome M. Gess, TAPPI Press, Atlanta, Third edition edn., 2005, ch. 14, pp. 257-286.
13. I. M. T. Moutinho, A. M. Kleen, M. M. L. Figueiredo and P. J. T. Ferreira, *Holzforschung*, 2009, **63**, 282-289.
14. J. Xu and H. Hu, *Journal of Applied Polymer Science*, 2012, **123**, 611-616.
15. C. M. Andersson and L. Järnström, *Appita Journal*, 2006, **59**, 207-212.
16. J. Sajbel, in *The Sizing of Paper*, ed. J. M. R. Jerome M. Gess, Tappi Press, Atlanta, Third edition edn., 2005, ch. 15, pp. 287-300.
17. R. Exner, *Paper Technology*, 2002, **43**, 45-51.
18. I. M. T. Moutinho, P. J. T. Ferreira and M. L. Figueiredo, *BioResources*, 2011, **6**, 4259-4270.
19. P. Wilson, in *The Sizing of Paper*, ed. J. M. R. Jerome M. Gess, Tappi Press, Atlanta, Third edition edn., 2005, ch. 13, pp. 249-256.
20. R. Carceller and A. Juppo, *Paperi ja Puu/Paper and Timber*, 2004, **86**, 161-163.
21. J. Gregory, *Advances in Colloid and Interface Science*, 2009, **147-148**, 109-123.
22. C. E. Barnett, *The Journal of Physical Chemistry*, 1942, **46**, 69-75.
23. O. Nechyporchuk, M. N. Belgacem and F. Pignon, *Cellulose*, 2015, **22**, 2197-2210.

24. G. Beaucage, *J. Appl. Crystallogr.*, 1995, **28**, 717-728.
25. R. J. Hunter, *Journal*, 2001, 380-381.
26. R. J. Hunter, *Journal*, 2001, 241.
27. B. Kronberg, K. Holmberg and B. Lindman, *Surface Chemistry of Surfactants and Polymers*, John Wiley & Sons, Ltd, 2014.
28. T. T. A. o. t. P. a. P. Industry), *Journal*, 2013.
29. S. Chakraborty, B. Sahoo, I. Teraoka and R. A. Gross, *Carbohydr. Polym.*, 2005, **60**, 475-481.
30. K. Schätzel and J. Merz, *J. Chem. Phys.*, 1984, **81**, 2482-2488.
31. K. Böckenhoff and W. R. Fischer, *Fresenius' Journal of Analytical Chemistry*, 2001, **371**, 670-674.
32. R. Wäsche, M. Naito and V. A. Hackley, *Powder Technol.*, 2002, **123**, 275-281.
33. W. Brown, *Dynamic light scattering: the method and some applications.* , Clarendon Press, Oxford, 1993.
34. R. L. Kearney, in *The Sizing of Paper*, ed. J. M. R. Jerome M. Gess, Tappi Press, Atlanta, Third edition edn., 2005, ch. 12, pp. 237-248.
35. X. Chen, J. Zhang, Z. Yi, Q. Wang, X. Li, F. Bian, J. Wang and Y. Men, *Journal of Coatings Technology Research*, 2011, **8**, 489-496.
36. C. W. H. John A. Lloyd, *Nordic Pulp & Paper Research Journal*, 1993, **8**.
37. J. J. M. Swinkels, *Starch - Stärke*, 1985, **37**, 1-5.
38. D. Kuakpetoon and Y. J. Wang, *Starch - Stärke*, 2001, **53**, 211-218.
39. D. Kuakpetoon and Y. J. Wang, *Carbohydr. Res.*, 2006, **341**, 1896-1915.
40. A. Fuchs and E. Killmann, *Colloid. Polym. Sci.*, 2001, **279**, 53-60.
41. G. Gillies, W. Lin and M. Borkovec, *J. Phys. Chem. B*, 2007, **111**, 8626-8633.
42. J. Gregory, *J. Colloid Interface Sci.*, 1973, **42**, 448-456.
43. J. Gregory, *J. Colloid Interface Sci.*, 1976, **55**, 35-44.
44. W. L. Yu, F. Bouyer and M. Borkovec, *J. Colloid Interface Sci.*, 2001, **241**, 392-399.
45. G. Carlsson and J. Van Stam, *Nord. Pulp. Pap. Res. J.*, 2005, **20**, 192-199.
46. N. P. Birch and J. D. Schiffman, *Langmuir*, 2014, **30**, 3441-3447.
47. L. Štajner, J. Požar and D. Kovačević, *Colloids Surf., A*, 2015, **483**, 171-180.
48. E. S. Dragan and S. Schwarz, *Journal of Polymer Science, Part A: Polymer Chemistry*, 2004, **42**, 5244-5252.
49. C. Ankerfors, S. Ondaral, L. Wågberg and L. Ödberg, *Journal of Colloid and Interface Science*, 2010, **351**, 88-95.
50. D. Kunz, A. Thurn and W. Burchard, *Colloid & Polymer Science*, 1983, **261**, 635-644.
51. H. W. Walker and S. B. Grant, *Colloids Surf., A*, 1996, **119**, 229-239.

52. A. Sadeghpour, E. Seyrek, I. Szilaźgyi, J. Hierrezuelo and M. Borkovec, *Langmuir*, 2011, **27**, 9270-9276.
53. J. Gregory and I. Sheiham, *British Polymer Journal*, 1974, **6**, 47-59.
54. E. G. M. Pelssers, M. A. C. Stuart and G. J. Fleer, *Colloids and Surfaces*, 1989, **38**, 15-25.
55. S. A. H. R.S. Anderssen, R.J. Loy, *Anziam journal*, 2004, **45**, C800-C816.
56. R. M. Syamaladevi, G. V. Barbosa-Cánovas, S. J. Schmidt and S. S. Sablani, *Carbohydrate Polymers*, 2012, **88**, 223-231.
57. S. Yoshioka, Y. Aso and S. Kojima, *Pharmaceutical Research*, 2001, **18**, 256-260.
58. W. A. De Morais, M. R. Pereira and J. L. C. Fonseca, *Carbohydrate Polymers*, 2012, **87**, 2376-2380.
59. V. A. V. De Oliveira, W. A. De Morais, M. R. Pereira and J. L. C. Fonseca, *European Polymer Journal*, 2012, **48**, 1932-1939.
60. Q. H. Yang, C. J. Qian, H. Li and M. B. Luo, *Physical Chemistry Chemical Physics*, 2014, **16**, 23292-23300.
61. T. W. Healy and V. K. La Mer, *Journal of Colloid Science*, 1964, **19**, 323-332.
62. F. Mabire, R. Audebert and C. Quivoron, *J. Colloid Interface Sci.*, 1984, **97**, 120-136.
63. Y. Shin, J. E. Roberts and M. M. Santore, *J. Colloid Interface Sci.*, 2002, **247**, 220-230.
64. K. Furusawa, M. Kanesaka and S. Yamashita, *J. Colloid Interface Sci.*, 1984, **99**, 341-348.
65. J. Zhang, C. Huguenard, C. Scarnecchia, R. Menghetti and J. Buffle, *Colloids Surf., A*, 1999, **151**, 49-63.
66. S. Schwarz, H. M. Buchhammer, K. Lunkwitz and H. J. Jacobasch, *Colloids Surf., A*, 1998, **140**, 377-384.
67. Y. Chen, S. Liu and G. Wang, *Chem. Eng. J.*, 2007, **133**, 325-333.
68. R. J. Hunter, *Journal*, 2001, 616-617.
69. J. Gregory and S. Barany, *Advances in Colloid and Interface Science*, 2011, **169**, 1-12.
70. J. A. De Witt and T. G. M. Van De Ven, *Langmuir*, 1992, **8**, 788-793.
71. I. M. T. Moutinho, P. J. T. Ferreira and M. L. Figueiredo, *Industrial and Engineering Chemistry Research*, 2007, **46**, 6183-6188.